ehp ENVIRONMENTAL HEALTH PERSPECTIVES
http://www.ehponline.org

Bidirectional Transfer Study of Polystyrene Nanoparticles across the Placental Barrier in an *ex Vivo* Human Placental Perfusion Model

Stefanie Grafmueller, Pius Manser, Liliane Diener, Pierre-André Diener, Xenia Maeder-Althaus, Lionel Maurizi, Wolfram Jochum, Harald F. Krug, Tina Buerki-Thurnherr, Ursula von Mandach, and Peter Wick

http://dx.doi.org/10.1289/ehp.1409271

Received: 29 September 2014
Accepted: 5 May 2015
Advance Publication: 8 May 2015

Environ Health Perspect doi: 10.1289/ehp.1409271
Advance Publication: Not Copyedited

Bidirectional Transfer Study of Polystyrene Nanoparticles across the Placental Barrier in an *ex Vivo* Human Placental Perfusion Model

Stefanie Grafmueller,[1,2,3] Pius Manser,[1] Liliane Diener,[1] Pierre-André Diener,[4] Xenia Maeder-Althaus,[1] Lionel Maurizi,[5] Wolfram Jochum,[4] Harald F. Krug,[6] Tina Buerki-Thurnherr,[1] Ursula von Mandach,[2] and Peter Wick[1]

[1]Laboratory for Particles-Biology Interactions, Empa, St. Gallen, Switzerland; [2]Perinatal Pharmacology, Department of Obstetrics, University Hospital Zurich, Zurich, Switzerland; [3]Graduate School for Cellular and Biomedical Sciences, University of Berne, Berne, Switzerland; [4]Institute of Pathology, Cantonal Hospital St. Gallen, St. Gallen, Switzerland; [5]Powder Technology Laboratory, Ecole Polytechnique Federale de Lausanne, Lausanne, Switzerland; [6]Empa, International Research Cooperations Manager, St. Gallen Switzerland

Address correspondence to Peter Wick, Empa, Swiss Federal Laboratories for Materials Science and Technology, Laboratory for Particles-Biology Interactions, Lerchenfeldstrasse 5, 9014 St. Gallen, Switzerland. Telephone: +41 58 765 76 84. E-mail: peter.wick@empa.ch

Running title: Placental transfer of polystyrene nanoparticles

Acknowledgments: This work was financially supported by the Swiss National Foundation, (NRP 64 program, grant no 4064-131232). This project has received funding from the European Union's Seventh Framework Programme for research, technological development and demonstration under grant agreement no 263215 (MARINA) and no 309329 (NANOSOLUTIONS).

We thank M. Roesslein for technical support in measurement of particle size distribution.

Competing financial interests: The authors declare that they have no competing financial interests.

Abstract

Background: Nanoparticle exposure *in utero* might not be a major concern yet, but could become more important with the increasing application of nanomaterials in consumer and medical products. Several epidemiologic and *in vitro* studies have shown that nanoparticles can have potential toxic effects. However, nanoparticles also offer the opportunity to develop new therapeutic strategies to treat specifically either the pregnant mother or the fetus. Previous studies mainly addressed whether nanoparticles are able to cross the placental barrier or not. Though, the transport mechanisms underlying nanoparticle translocation across the placenta are still unknown.

Objectives: In this study we examined which transport mechanisms underlie the placental transfer of nanoparticles.

Methods: We used the *ex vivo* human placental perfusion model to analyze the bidirectional transfer of plain and carboxylate modified polystyrene particles in a size range between 50 to 300 nm.

Results: We showed that the transport of polystyrene particles in the fetal to maternal direction was significantly higher than for the maternal to fetal direction. Regardless of their ability to cross the placental barrier and the direction of perfusion, all polystyrene particles accumulated in the syncytiotrophoblast of the placental tissue.

Conclusions: Our results indicate that the syncytiotrophoblast is the key player in regulating nanoparticle transport across the human placenta. The main mechanism underlying this translocation is not based on passive diffusion, but is likely to involve an active, energy-dependent transport pathway. These findings will be important for reproductive toxicology as well as for pharmaceutical engineering of new drug carriers.

Introduction

Currently the application of engineered nanoparticles (NP) in industrial and consumer products is increasing continuously. Epidemiological as well as *in vitro* studies showed that engineered, naturally occurring as well as combustion-derived NPs could have adverse health effects in humans (Bell et al. 2012; Pietroiusti 2012). However, to cause damage *in vivo*, NPs have to cross highly protective biological barriers. Besides the intestine and skin, the air-blood barrier of the lung is an important entry site for NPs. Multiple studies have shown that NPs are able to cross this protective barrier *in vitro* and *in vivo* (Geiser et al. 2005; Kreyling et al. 2009; Rothen-Rutishauser et al. 2007). Furthermore, NPs are applied in various medical products like contrast agents for imaging or metal oxide particles for cancer therapy (Gupta and Gupta 2005; Rasmussen et al. 2010). Since these medical NPs need to be injected, they get direct access to the blood circulation. Therefore it will be increasingly important to investigate NP transport across internal barriers such as the placenta barrier between the mother and the unborn child.

The placenta is responsible for the supply of nutrients, the removal of waste products and the protection of the fetus against harmful substances. It is organized in cotyledons, which represent the functional units of the placenta. Each cotyledon is formed by a fetal villous tree. Due to the extensive division of the villous trees the total exchange surface area at term is about 13 m^2 (Larsen et al. 1995; Syme et al. 2004). The maternal blood is released into the intervillous space and separated from the fetal circulation by the syncytiotrophoblast layer, some few cytotrophoblast cells and the endothelial cell layer of the fetal capillaries, which are surrounded by stromal fibroblasts and fetal macrophages. The thickness of this barrier decreases during pregnancy to allow an increased maternal-fetal exchange at late gestational ages (Juch et al.

2013; Syme et al. 2004). The syncytiotrophoblast layer as key barrier is built from cytotrophoblast cells which fuse during development and form a true syncytium without lateral cell membranes (Enders and Blankenship 1999). The plasma membrane of the syncytiotrophoblast is highly polarized and consists of two membranes. The basal membrane is in contact with the villous stroma which surrounds the fetal capillaries while the brush border membrane with its many microvilli faces the maternal blood stream. The polarity of the syncytiotrophoblast is based on a different repertoire of transport proteins for each of these membranes. Furthermore, there is a huge variety of transporters, which act in both directions (importer and exporter), to ensure an optimal supply with nutrients and an efficient efflux of waste products or harmful drugs (Ganapathy et al. 2000). The placental transfer of such substances depends on four different mechanisms: passive diffusion, active transport, phagocytosis/ pinocytosis and biotransformation through metabolic enzymes (Syme et al. 2004).

Several animal studies showed that different NPs like gold, silica or titanium dioxide can cross the placental barrier and some of them can even impair fetal development (Semmler-Behnke et al. 2008; Yamashita et al. 2011). However, the placenta is the most species-specific organ and data obtained in rodent models cannot be simply extrapolated to the human system (Enders and Blankenship 1999; Takata and Hirano 1997). The *ex vivo* human placental perfusion provides an ethically accepted model, close to the *in vivo* situation, to investigate placental transport of xenobiotics as well as NPs (Grafmuller et al. 2013; Malek et al. 2009; Panigel et al. 1967; Schneider et al. 1972). Using this model it has been shown that 25 and 50 nm silica particles are transported across the human placental barrier while pegylated 10 – 30 nm gold particles were retained in the maternal circulation and the placental tissue (Myllynen et al. 2008; Sonnegaard

Poulsen et al. 2013). Previous work performed by our group revealed a size-dependent translocation of polystyrene (PS) particles with placental passage of PS particles up to 240 nm in diameter (Wick et al. 2010). Though there is an increasing number of *in vivo* and *in vitro* studies about placental NP transport (Buerki-Thurnherr et al. 2012; Saunders 2009), the transport mechanisms for NPs across the placental barrier are largely unknown. Knowledge about the route of NP transport across the placenta barrier and about its dependency on NPs physicochemical properties is a prerequisite for future development of NPs as drug carriers to either specifically treat the mother without affecting the fetus or even to treat placental dysfunctions. Additionally, a better understanding of the translocation of NPs across an internal barrier such as the placenta would also contribute to a safer design of NPs in general. To assess the contribution of the physicochemical properties of NPs to placental NP transfer and the transport mechanisms underlying this process, we performed and analyzed bidirectional transfer studies of fluorescently labeled PS particles with different sizes and surface modifications in the *ex vivo* human placental perfusion model.

Materials and Methods

Particles

Yellow-green-labeled PS beads without functionalization (plain) with the size of 50 and 240 nm from Spherotech were used. Yellow-green-labeled, carboxylate-modified (COOH) 50 and 300 nm PS beads were purchased from Polysciences, Inc.

Particle characterization

The zeta potential in 10 mM sodium chloride and perfusion medium at pH between 6.8 and 7.2 was determined with a Zetasizer NanoZS (Malvern Instruments).

Particle size distribution in double distilled (DD) water and perfusion medium (PM) was determined by nanoparticle tracking analysis (NTA; NanoSight LM 20 System, software version 2.3, NanoSight Ltd.) as described previously (Hole et al. 2013). The composition of the PM is described in the Supplemental Material, section *ex vivo* human placental perfusion model. The DD water and PM were filtered through a 0.02 µm Anotop® 25 syringe filter (Whatman GmbH) prior to analysis. For each particle size the results were normalized to the area under the NP concentration/size curve.

The detection limit of the PS beads fluorescence was determined by making a serial dilution in the range of 0.02 – 10 µg/mL of each PS particle in perfusion medium. The detection limit was defined as the minimum concentration of PS particles in perfusion medium which showed a significant increase in fluorescence intensity as compared to pure perfusion medium.

To assess the stability of fluorescence the loss of fluorescence intensity was analyzed after incubation of the PS beads in perfusion medium at 37 °C for 3, 6, 24, 48 and 72 hrs using a microplate reader (Biotek Synergy HT) with excitation and emission wavelengths of 485 and 528 nm. The leakage of fluorescence was assessed by measuring the fluorescence before and after filtration through a 0.1 µm syringe filter at the end of the indicated incubation periods.

Cell culture

BeWo cells (b30 clone), a cell line derived from human choriocarcinoma, were obtained from Prof. Dr. Ursula Graf-Hausner (Zurich University of Applied Sciences, Waedenswil, Switzerland) with permission of Dr. Alan L. Schwartz (Washington University School of Medicine, MO, USA) and cultured in Ham´s F-12K medium (Gibco, Thermo Fisher Scientific

Inc.) supplemented with 1 % penicillin-streptomycin and 10 % fetal calf serum (FCS) at 37°C and 5 % carbon dioxide (CO_2).

MTS viability assay

The *in vitro* cytotoxicity of the different PS beads was tested using the MTS viability assay. 24 hrs before treatment BeWo cells were seeded in a 96-well plate (8000 cells per well). Different concentrations of PS beads were applied. As negative control, cells without treatment were used and as positive control 1, 10, 100 and 1000 µM $CdSO_4$ was applied. After 3 or 24 hrs of incubation at 37 °C and 5 % CO_2, an MTS assay (CellTiter96® AQ_{ueous} One Solution Cell Proliferation Assay; Promega) was performed according to the manufacturer's instructions. Results were presented as mean percentage of the untreated control from three independent experiments.

Viability and functionality, antipyrine transfer and histopathological evaluation of placental tissue

Glucose and lactate concentration in the fetal and maternal circuit were determined as indicators for tissue viability. The placenta hormones human chorionic gonadotropin (hCG) and leptin production were estimated to assess tissue functionality. Tissue samples of non-perfused and perfused placentas were fixed and examined by light microscopy. Detailed work procedures are available in the Supplemental Material.

Ex vivo human placental perfusion model

The placentas were obtained from uncomplicated term pregnancies after caesarean section at the Department of Obstetrics at the University Hospital Zurich, the Kantonsspital and the Klinik Stephanshorn in St. Gallen. Written informed consent was obtained prior to delivery. The project

was approved by the local ethics committee and performed in accordance with the principles of the Declaration of Helsinki. The placenta perfusion was performed as described previously (Grafmuller et al. 2013; Wick et al. 2010). For a brief description see Supplemental Material, section *ex vivo* human placenta perfusion model.

Fluorescence microscopy

Unstained paraffin sections of non-perfused (negative control) and perfused placenta were deparaffinized with xylene followed by 100 % ethanol. Afterwards the slides were air-dried, covered with VECTASHIELD® Mounting Medium containing DAPI (Vector Laboratories) on a glass slide and the coverslips were sealed with nail polish. The slides were analysed with a Leica DM6000B fluorescence microscope system (Leica Microsystems) equipped with a triple band pass filter set (DAPI/Spectrum Green/Spectrum Orange).

Transmission electron microscopy (TEM)

Particle suspensions as supplied by the manufacturer were applied onto a carbon-coated copper grid and processed for TEM analysis (Zeiss 900 TEM, Carl Zeiss MicroImaging). Samples from fetal or maternal circulation after 1.5 - 6 hrs of perfusion were centrifuged twice for 30 minutes at 25000 x *g* and 4 °C. The pellets were resuspended in DD water and processed for TEM analysis as described for the particle suspensions.

Statistical analysis

Data are shown as mean ± standard deviation (SD) from at least three independent experiments. Unpaired Student's t-test was performed using GraphPad Prism software, version 6 (GraphPad Software). Differences were considered statistically significant at a p-value below 0.05.

Results

Particle characterization and cytotoxicity evaluation

The fluorescently labeled PS beads were extensively characterized and the results are summarized in Table 1 and Figure 1. All PS particles suspended in 10 mM sodium chloride solution were negatively charged, but the zeta potential of the carboxylate-modified PS beads was significantly lower than the one of plain PS beads in the same size range. Analysis of the size distribution by nanoparticle tracking analysis confirmed that the plain 50 nm and carboxylate-modified 50 nm PS beads were relatively monodisperse (Figure 1A, B). However, the plain 240 nm and carboxylate-modified 300 nm PS beads contained an additional fraction of smaller beads around 100 nm which were not observed to that extent in the corresponding TEM micrographs (Figure 1D, F). Furthermore, TEM images demonstrated that the plain and carboxylate-modified 50 nm PS beads contained some smaller particles of around 20 nm in diameter (Figure 1C, E). As expected, the hydrodynamic diameter for all PS beads in perfusion medium was higher than in water (Table 1).

Since a few studies showed a leakage of the fluorescence dye from NPs (Pietzonka et al. 2002; Tenuta et al. 2011), their stability in perfusion medium was tested over a time period of 72 hrs at 37 °C. After 3 hrs fluorescence intensity decreased to 75 ± 4 % of the initial signal for the plain 50 nm, 76 ± 2 % for the plain 240 nm, 83 ± 4 % for the carboxylate-modified 50 nm and 84 ± 5 % for the carboxylate-modified 300 nm PS beads, but then remain stable up to 72 hrs (see Supplemental Material, Figure S1A). This slight decrease in fluorescence intensity was not due to a loss of fluorescence dye from the particles, as mean leakage of the dye was below 0.52 % for the plain 240 nm and 2.3 % for the carboxylate-modified 300 nm PS beads (see Supplemental

Material, Figure S1B). Filtration of the smaller beads through a 20 nm syringe filter was attempted, but failed due to the high viscosity of the perfusion medium and the obstruction of the filter. Therefore leakage of the dye could not be assessed in these samples.

To confirm the absence of cytotoxic effects of the PS beads an MTS viability assay was performed on BeWo cells. These cells were used as a model of the syncytiotrophoblast which got into contact with the NPs in the *ex vivo* perfusion system first. None of the PS particles significantly decreased cell viability even at higher concentrations and longer exposure time than those used in the *ex vivo* perfusion experiments (see Supplemental Material, Figure S2).

Placental transfer

In a previous study we observed a size-dependent transfer of PS beads after 3 hrs of *ex vivo* human placental perfusion in maternal to fetal direction with the highest transfer rate for plain 50 nm PS beads (Wick et al. 2010). In the current study we investigated the bidirectional placental transfer of plain 50 and 240 nm as well as carboxylate-modified 50 and 300 nm PS particles by either adding 25 µg/mL PS beads to the maternal (M) or to the fetal (F) circulation. After 6 hrs of perfusion, the concentration of all PS beads was increased in reverse direction (F to M) as compared to normal perfusions (M to F direction) (Figure 2A - D). We observed a significant difference in placental transfer between normal and reverse perfusions for the plain 50 nm (M to F 13.7 ± 8.4 % versus F to M 23.7 ± 5.8 %), the carboxylate-modified 50 nm (M to F 1.4 ± 0.5 % versus F to M 7.2 ± 1.3 %) and carboxylate-modified 300 nm PS beads (M to F 1.2 ± 0.7 % versus F to M 5.3 ± 0.5 %) (Figure 2E). Plain 240 nm PS beads also showed a tendency for a higher transfer in the reverse direction (M to F 2.4 ± 0.7 % versus F to M 6.1 ± 4.1 %) indicating a generally increased placental permeability in the F to M direction. In addition, we showed an

increased translocation of non-functionalized 50 nm PS beads as compared to carboxylate-modified 50 nm PS particles in both directions indicating that the surface charge or modification of NPs could also influence placental NP transfer (Figure 2A, C, E). For the particles in the size range between 240 and 300 nm a significant difference between plain and carboxylate-modified beads was also observed but only in perfusions from M to F direction (Figure 2B, D, E). To ensure that we did not measure placental transfer of detached fluorescence dye, we wanted to recover the PS beads from the fetal (in case of normal perfusions) or the maternal (reverse perfusions) perfusates after *ex vivo* perfusion. In TEM micrographs both large (240 and 300 nm) and the plain 50 nm PS beads were found in the maternal perfusate after reverse perfusions, whereas in the fetal perfusate after normal perfusions only the plain 50 nm PS beads were detected (see Supplemental Material, Figure S1C). Transfer of the plain 240 nm and both carboxylate-modified beads from M to F direction was too low (< 0.8 µg/mL) for detection by TEM, but still within the detection limit of the more sensitive fluorescence measurement. Moreover, during *ex vivo* placental perfusion a great amount of other electron dense substances such as proteins or sugars were released in both circulations, which made it especially difficult to find the small 50 nm PS beads via TEM analysis. Therefore, only the plain 50 nm PS beads were detectable in TEM micrographs due to their high transfer in both directions.

As control for a passively transported substance across the placental barrier, radiolabeled ^{14}C-antipyrine was added to each perfusion. After 4 - 6 hrs equal concentrations should be reached in both circulations (Challier et al. 1983) and F to M or M to F concentration ratios should be around 1. This criterion was fulfilled in all perfusions demonstrating that the PS beads had no effect on barrier permeability itself (see Supplemental Material, Figure S3A, B). Of note,

the development of the concentration equilibrium of antipyrine in reverse perfusions was decelerated compared to perfusions in M to F direction (see Supplemental Material, Figure S3A, B). During the perfusion process there was no influence of the PS beads on viability (glucose consumption and lactate production) and functionality (human chorionic gonadotropin and leptin secretion) of the placenta (see Supplemental Material, Figure S3C, D). Moreover, no visible structural changes to the placental tissue after perfusion with or without particles were identified in histological tissue sections (data not shown).

Despite there was only little transfer of the plain 240 nm, carboxylate-modified 50 nm and 300 nm PS beads in both directions, the maternal (normal perfusions) or fetal (reverse perfusions) concentration of these beads was declining (Figure 2B, C, D). Fluorescence microscopic images showed that these particles accumulated in the placental tissue (Figure 3). PS beads were mainly found in the syncytiotrophoblast layer of the placental villi independent of particle size, functionalization or mode of perfusion (Figure 3A, B). Unfortunately a reliable quantification of the PS beads in the tissue based on the fluorescence images was not possible because resolution is not sufficient to visualize single particles and small agglomerates which would lead to an underestimation of NP tissue content. Therefore we calculated the theoretical amount of PS beads in the tissue by subtracting the measured concentration in the fetal and maternal circuit from the initially added concentration (Figure 3C). After 6 hrs of perfusion the tissue content of the PS beads with a higher transfer rate (plain 50 nm F to M and M to F; plain 240 nm F to M; COOH 300 nm F to M) was significantly lower as compared to the PS beads (COOH 50 nm M to F and F to M; plain 240 nm M to F, COOH 300 nm M to F) with only low placental transfer (Figure 3C).

Discussion

In this study we showed a bidirectional transfer of plain and carboxylate-modified PS beads up to a size of 300 nm using the *ex vivo* human placental perfusion model. The placental transport was increased in reverse perfusions from the fetal to the maternal side indicating that there are different transport mechanisms for PS particles on the fetal and maternal side of the human placenta. Although transport in the reverse direction is physiologically not relevant regarding *in vivo* exposure to NPs, which will only occur in the maternal circulation, reverse *ex vivo* placental perfusion is a common method to evaluate the mode of transport of many drugs across the human placenta (Nanovskaya et al. 2012; Nekhayeva et al. 2005; Sudhakaran et al. 2005). For example a study about bidirectional placental transfer of antibiotics revealed that telavancin has a higher placental transfer in the reverse direction suggesting a translocation not simply by passive diffusion, but indicates that specific transporters may be involved (Nanovskaya et al. 2012). However, it is rather unlikely that NPs in general are transported via such transporters across the placenta (Menezes et al. 2011). Nevertheless our results demonstrate that passive diffusion is not the key mechanism underlying placental translocation of PS particles, because concentration equilibrium was not achieved after 4 – 6hours as compared to the passively transported antipyrine. According to Fick's law, diffusion of a substance mainly depends on the permeability of the membrane for this substance, the concentration gradient across the membrane and the membrane surface area. In our study placental transfer kinetics of antipyrine from F to M direction was significantly delayed as compared to M to F direction which was likely due to the lower exchange surface on the fetal side (inner surface of the fetal capillaries compared to the very large brush border membrane of the syncytiotrophoblast on the maternal side) and the reduced fetal perfusion flow (3 - 4 mL/min compared to 12 mL/min for the maternal circuit) (Challier et al. 1983). Thus, NP trans-

fer in the reverse direction should be reduced if it would be based predominantly on a passive transport mechanism. Opposite to such an expectation, we observed an augmented transfer in F to M direction (compared to M to F) of PS particles independent of their physicochemical properties, suggesting an energy-dependent transport mechanism for PS particle translocation across the human placenta. Phagocytosis is one example of an energy-dependent mechanism proposed for NP uptake into cells especially in phagocytes (Jud et al. 2013). It has been shown that primary human macrophages engulf carboxylate-modified PS beads via this pathway whereas THP-1 cells, a human monocytic leukemia cell line, use an endocytosis pathway (Lunov et al. 2011). During phagocytosis vesicles with a diameter > 0.5 μm are formed, whereas the diameter of endocytotic vesicles is considerably smaller (Aderem and Underhill 1999). Caveolin coated vesicles are defined as membrane invaginations with a diameter of 60 to 80 nm and vesicles arising from clathrin-dependent endocytosis are described to have a diameter of approximately 120 to 150 nm e.g. in human epithelial cells (McMahon and Boucrot 2011; Parton and Simons 2007). A study using specific transport pathway inhibitors revealed that A549 cells, a human alveolar epithelial cell line, take up gold NPs with a diameter of 15 nm mainly by endocytosis (Brandenberger et al. 2010). Moreover, endo- and transcytosis are also proposed as the most common transport mechanisms for NPs at the blood-brain barrier (Kreuter 2014).

Most of the studies about NP uptake mechanism were performed on non-polarized cells or cell lines, which do not resemble a typical polarized barrier as the placental syncytiotrophoblast. The different membrane properties and receptor repertoires on the apical and basal side may allow different transport mechanisms depending on the site of exposure. So far most groups observed NP uptake in the syncytiotrophblast after *ex vivo* human placental perfusion even if NP translo-

cation to the fetal circulation was absent or below detection limit (Menjoge et al. 2011; Myllynen et al. 2008; Sonnegaard Poulsen et al. 2013). We also observed most of the PS particles accumulated predominantly in the syncytiotrophoblast layer, which indicates that the syncytium is a major determinant of NP transfer. Besides the syncytiotrophoblast the endothelial cells of the fetal capillaries are also part of the placental barrier. It has been shown that these cells contribute to the barrier function and mostly act as a molecular sieve for larger hydrophilic molecules (Firth and Leach 1996). However, to evaluate the definite contribution of the fetal endothelium to placental NP transfer, *in vitro* co-culture models including trophoblasts as well as endothelial cells are necessary and currently under development (Levkovitz et al. 2013).

Nanoparticle uptake into cells also depends on the physicochemical properties of the materials (Lunov et al. 2011). We demonstrated that carboxylate-modified PS beads were transferred across the placenta in significantly lower amounts than plain particles. The carboxylate-modified PS beads had a lower zeta potential than the plain beads indicating that the surface charge of NPs can have an impact on placental transfer. Indeed, such a surface charge-dependent placental translocation has been demonstrated in pregnant rats where amine-modified PS beads showed a stronger translocation than carboxylate-modified PS beads (Tian et al. 2009). Similar observations have been made with NPs at other biological barriers. The accumulation of negatively charged gold NPs in secondary organs after oral exposure in rats was higher than for positively charged particles (Schleh et al. 2012). Furthermore, studies of NP uptake at the air-blood barrier revealed that the surface charge of NPs below a size threshold of 34 nm is the most critical factor for translocation (Choi et al. 2010). Differently charged NPs acquire a distinct protein corona after contact with serum or biological fluids (Hirsch et al. 2013; Lundqvist et al. 2008; Monopoli et

al. 2011). The protein corona can influence the biological fate of NPs through alteration of their hydrodynamic diameter or surface properties. In addition, serum proteins can also influence directly the uptake mechanism of NPs by binding to their specific receptors on the cell surface, thereby mediating endocytosis (Monopoli et al. 2012). Several groups observed that albumin concentration in the perfusion medium determines the transplacental transfer of several drugs in the *ex vivo* human placental perfusion model (Mathiesen et al. 2009; Nanovskaya et al. 2008). The perfusion medium used in our study was supplemented with albumin only and not with complete serum. However, many other proteins are produced by placental cells during perfusion and are released into the circulation where they can get in contact with the PS beads. Interestingly, many hormones produced in the placenta are secreted asymmetrically into the maternal and the fetal circulation (Linnemann et al. 2000; Malek et al. 2001). Therefore adsorption of different proteins in fetal and maternal circulation may also provide an explanation for the differential transport in normal and reverse perfusions in our study. To corroborate this hypothesis, further studies with a broad variety of differently charged NPs as well as on the composition of the NP protein corona are required.

Studies using the *ex vivo* human placental perfusion model are limited to a few hours of perfusion due to tissue degradation (Panigel et al. 1967; Schneider et al. 1972), and only reflect placental transport at late pregnancy. To assess long-term effects of NP exposure and transport during early stages of pregnancy, when the placental barrier is much thicker (Nikitina et al. 2013), *in vitro* studies are indispensable. In addition, *in vitro* studies would allow a higher throughput than *ex vivo* perfusions. So, involvement of specific transport pathways could be tested first *in vitro* and could be subsequently confirmed in the *ex vivo* placental perfusion model which is closer to

the *in vivo* situation. Overall, development of more advanced and carefully validated *in vitro* models, which include also flow and several placental cell types, are expected to lead to a better understanding of NP transport mechanisms across the placental barrier and their dependence on the physicochemical properties of NPs.

Conclusions

To our knowledge this is the first approach to investigate the transport mechanism of NPs by studying bidirectional transfer of PS particles in the *ex vivo* human placental perfusion model. We demonstrated an increased transfer of PS beads in reverse (F to M direction) perfusions and an accumulation of PS beads in the syncytiotrophoblast layer of the placental tissue. Based on our findings we can exclude a transfer via passive diffusion. We propose an energy-dependent placental translocation pathway and the polarized syncytiotrophoblast as the main contributor to NP transfer in the placenta. Though, for the development and the safe use of NPs in nanomedicine, transport mechanisms of NPs across the placental barrier need to be determined precisely in further studies.

References

Aderem A, Underhill DM. 1999. Mechanisms of phagocytosis in macrophages. Annu Rev Immunol 17:593-623.

Bell ML, Belanger K, Ebisu K, Gent JF, Leaderer BP. 2012. Relationship between birth weight and exposure to airborne fine particulate potassium and titanium during gestation. Environ Res 117:83-89.

Brandenberger C, Muhlfeld C, Ali Z, Lenz AG, Schmid O, Parak WJ, et al. 2010. Quantitative evaluation of cellular uptake and trafficking of plain and polyethylene glycol-coated gold nanoparticles. Small 6:1669-1678.

Buerki-Thurnherr T, von Mandach U, Wick P. 2012. Knocking at the door of the unborn child: Engineered nanoparticles at the human placental barrier. Swiss Med Wkly 142:w13559.

Challier JC, D'Athis P, Guerre-Millo M, Nandakumaran M. 1983. Flow-dependent transfer of antipyrine in the human placenta in vitro. Reprod Nutr Dev 23:41-50.

Choi HS, Ashitate Y, Lee JH, Kim SH, Matsui A, Insin N, et al. 2010. Rapid translocation of nanoparticles from the lung airspaces to the body. Nat Biotechnol 28:1300-1303.

Enders AC, Blankenship TN. 1999. Comparative placental structure. Adv Drug Deliv Rev 38:3-15.

Firth JA, Leach L. 1996. Not trophoblast alone: A review of the contribution of the fetal microvasculature to transplacental exchange. Placenta 17:89-96.

Ganapathy V, Prasad PD, Ganapathy ME, Leibach FH. 2000. Placental transporters relevant to drug distribution across the maternal-fetal interface. J Pharmacol Exp Ther 294:413-420.

Geiser M, Rothen-Rutishauser B, Kapp N, Schurch S, Kreyling W, Schulz H, et al. 2005. Ultrafine particles cross cellular membranes by nonphagocytic mechanisms in lungs and in cultured cells. Environ Health Perspect 113:1555-1560.

Grafmuller S, Manser P, Krug HF, Wick P, von Mandach U. 2013. Determination of the transport rate of xenobiotics and nanomaterials across the placenta using the ex vivo human placental perfusion model. J Vis Exp 18:76.

Gupta AK, Gupta M. 2005. Synthesis and surface engineering of iron oxide nanoparticles for biomedical applications. Biomaterials 26:3995-4021.

Hirsch V, Kinnear C, Moniatte M, Rothen-Rutishauser B, Clift MJ, Fink A. 2013. Surface charge of polymer coated spions influences the serum protein adsorption, colloidal stability and subsequent cell interaction in vitro. Nanoscale 5:3723-3732.

Hole P, Sillence K, Hannell C, Maguire CM, Roesslein M, Suarez G, et al. 2013. Interlaboratory comparison of size measurements on nanoparticles using nanoparticle tracking analysis (nta). J Nanopart Res 15:2101.

Juch H, Nikitina L, Debbage P, Dohr G, Gauster M. 2013. Nanomaterial interference with early human placenta: Sophisticated matter meets sophisticated tissues. Reprod Toxicol 41:73-79.

Jud C, Clift MJ, Petri-Fink A, Rothen-Rutishauser B. 2013. Nanomaterials and the human lung: What is known and what must be deciphered to realise their potential advantages? Swiss Med Wkly 143:w13758.

Kreuter J. 2014. Drug delivery to the central nervous system by polymeric nanoparticles: What do we know? Adv Drug Deliv Rev 71:2-14.

Kreyling WG, Semmler-Behnke M, Seitz J, Scymczak W, Wenk A, Mayer P, et al. 2009. Size dependence of the translocation of inhaled iridium and carbon nanoparticle aggregates from the lung of rats to the blood and secondary target organs. Inhal Toxicol 21 Suppl 1:55-60.

Larsen LG, Clausen HV, Andersen B, Graem N. 1995. A stereologic study of postmature placentas fixed by dual perfusion. Am J Obstet Gynecol 172:500-507.

Levkovitz R, Zaretsky U, Gordon Z, Jaffa AJ, Elad D. 2013. In vitro simulation of placental transport: Part i. Biological model of the placental barrier. Placenta 34:699-707.

Linnemann K, Malek A, Sager R, Blum WF, Schneider H, Fusch C. 2000. Leptin production and release in the dually in vitro perfused human placenta. J Clin Endocrinol Metab 85:4298-4301.

Lundqvist M, Stigler J, Elia G, Lynch I, Cedervall T, Dawson KA. 2008. Nanoparticle size and surface properties determine the protein corona with possible implications for biological impacts. Proc Natl Acad Sci U S A 105:14265-14270.

Lunov O, Syrovets T, Loos C, Beil J, Delacher M, Tron K, et al. 2011. Differential uptake of functionalized polystyrene nanoparticles by human macrophages and a monocytic cell line. ACS Nano 5:1657-1669.

Malek A, Willi A, Muller J, Sager R, Hanggi W, Bersinger N. 2001. Capacity for hormone production of cultured trophoblast cells obtained from placentae at term and in early pregnancy. J Assist Reprod Genet 18:299-304.

Malek A, Obrist C, Wenzinger S, von Mandach U. 2009. The impact of cocaine and heroin on the placental transfer of methadone. Reprod Biol Endocrinol 7:61.

Mathiesen L, Rytting E, Mose T, Knudsen LE. 2009. Transport of benzo[alpha]pyrene in the dually perfused human placenta perfusion model: Effect of albumin in the perfusion medium. Basic Clin Pharmacol Toxicol 105:181-187.

McMahon HT, Boucrot E. 2011. Molecular mechanism and physiological functions of clathrin-mediated endocytosis. Nat Rev Mol Cell Biol 12:517-533.

Menezes V, Malek A, Keelan JA. 2011. Nanoparticulate drug delivery in pregnancy: Placental passage and fetal exposure. Curr Pharm Biotechnol 12:731-742.

Menjoge AR, Rinderknecht AL, Navath RS, Faridnia M, Kim CJ, Romero R, et al. 2011. Transfer of pamam dendrimers across human placenta: Prospects of its use as drug carrier during pregnancy. J Control Release 150:326-338.

Monopoli MP, Walczyk D, Campbell A, Elia G, Lynch I, Bombelli FB, et al. 2011. Physical-chemical aspects of protein corona: Relevance to in vitro and in vivo biological impacts of nanoparticles. J Am Chem Soc 133:2525-2534.

Monopoli MP, Aberg C, Salvati A, Dawson KA. 2012. Biomolecular coronas provide the biological identity of nanosized materials. Nat Nanotechnol 7:779-786.

Myllynen PK, Loughran MJ, Howard CV, Sormunen R, Walsh AA, Vahakangas KH. 2008. Kinetics of gold nanoparticles in the human placenta. Reprod Toxicol 26:130-137.

Nanovskaya T, Patrikeeva S, Zhan Y, Fokina V, Hankins GD, Ahmed MS. 2012. Transplacental transfer of vancomycin and telavancin. Am J Obstet Gynecol 207:331 e331-336.

Nanovskaya TN, Patrikeeva S, Hemauer S, Fokina V, Mattison D, Hankins GD, et al. 2008. Effect of albumin on transplacental transfer and distribution of rosiglitazone and glyburide. J Matern Fetal Neonatal Med 21:197-207.

Nekhayeva IA, Nanovskaya TN, Deshmukh SV, Zharikova OL, Hankins GD, Ahmed MS. 2005. Bidirectional transfer of methadone across human placenta. Biochem Pharmacol 69:187-197.

Nikitina L, Dohr G, Juch H. 2013. Studying nanoparticle interaction with human placenta: Festina lente! Nanotoxicology DOI: 10.3109/17435390.2013.859322.

Panigel M, Pascaud M, Brun JL. 1967. [radioangiographic study of circulation in the villi and intervillous space of isolated human placental cotyledon kept viable by perfusion]. J Physiol (Paris) 59:277.

Parton RG, Simons K. 2007. The multiple faces of caveolae. Nat Rev Mol Cell Biol 8:185-194.

Pietroiusti A. 2012. Health implications of engineered nanomaterials. Nanoscale 4:1231-1247.

Pietzonka P, Rothen-Rutishauser B, Langguth P, Wunderli-Allenspach H, Walter E, Merkle HP. 2002. Transfer of lipophilic markers from plga and polystyrene nanoparticles to caco-2 monolayers mimics particle uptake. Pharm Res 19:595-601.

Rasmussen JW, Martinez E, Louka P, Wingett DG. 2010. Zinc oxide nanoparticles for selective destruction of tumor cells and potential for drug delivery applications. Expert Opin Drug Deliv 7:1063-1077.

Rothen-Rutishauser B, Muhlfeld C, Blank F, Musso C, Gehr P. 2007. Translocation of particles and inflammatory responses after exposure to fine particles and nanoparticles in an epithelial airway model. Part Fibre Toxicol 4:9.

Saunders M. 2009. Transplacental transport of nanomaterials. Wiley Interdiscip Rev Nanomed Nanobiotechnol 1:671-684.

Schleh C, Semmler-Behnke M, Lipka J, Wenk A, Hirn S, Schaffler M, et al. 2012. Size and surface charge of gold nanoparticles determine absorption across intestinal barriers and accumulation in secondary target organs after oral administration. Nanotoxicology 6:36-46.

Schneider H, Panigel M, Dancis J. 1972. Transfer across the perfused human placenta of antipyrine, sodium and leucine. Am J Obstet Gynecol 114:822-828.

Semmler-Behnke M, Kreyling WG, Lipka J, Fertsch S, Wenk A, Takenaka S, et al. 2008. Biodistribution of 1.4- and 18-nm gold particles in rats. Small 4:2108-2111.

Sonnegaard Poulsen M, Mose T, Leth Maroun L, Mathiesen L, Ehlert Knudsen L, Rytting E. 2013. Kinetics of silica nanoparticles in the human placenta. Nanotoxicology DOI:10.3109/17435390.2013.812259.

Sudhakaran S, Ghabrial H, Nation RL, Kong DC, Gude NM, Angus PW, et al. 2005. Differential bidirectional transfer of indinavir in the isolated perfused human placenta. Antimicrob Agents Chemother 49:1023-1028.

Syme MR, Paxton JW, Keelan JA. 2004. Drug transfer and metabolism by the human placenta. Clin Pharmacokinet 43:487-514.

Takata K, Hirano H. 1997. Mechanism of glucose transport across the human and rat placental barrier: A review. Microsc Res Tech 38:145-152.

Tenuta T, Monopoli MP, Kim J, Salvati A, Dawson KA, Sandin P, et al. 2011. Elution of labile fluorescent dye from nanoparticles during biological use. PLoS One 6:e25556.

Tian F, Razansky D, Estrada GG, Semmler-Behnke M, Beyerle A, Kreyling W, et al. 2009. Surface modification and size dependence in particle translocation during early embryonic development. Inhal Toxicol 21 Suppl 1:92-96.

Wick P, Malek A, Manser P, Meili D, Maeder-Althaus X, Diener L, et al. 2010. Barrier capacity of human placenta for nanosized materials. Environ Health Perspect 118:432-436.

Yamashita K, Yoshioka Y, Higashisaka K, Mimura K, Morishita Y, Nozaki M, et al. 2011. Silica and titanium dioxide nanoparticles cause pregnancy complications in mice. Nat Nanotechnol 6:321-328.

Table 1. Summary of PS beads characteristics.

NP characteristics	Plain 50 nm	Plain 240 nm	COOH 50 nm	COOH 300 nm
Diameter (nm)[a]	49	240	42.5	302.7
Diameter (nm)[b] in TEM	43.7 ± 8	220.5 ± 5.1	44.1 ± 7.1	289.4 ± 10.2
Hydrodynamic diameter in DD water(nm)[c]	88 ± 79.5	230 ± 65.3	68 ± 19.2	283 ± 85.2
Hydrodynamic diameter in PM (nm)[c]	104 ± 74.7	273 ± 95.4	114 ± 49.1	359 ± 101.2
Initial no. of particles/mL in PM[d]	5.45E+11	4.24E+09	5.30E+11	1.88E+09
Particle surface (nm^2)/mL in PM[d]	3.27E+15	6.48E+14	3.24E+15	4.94E+14
Detection limit in PM (μg/mL)	< 1.25	< 0.63	< 0.078	< 0.078
Zeta potential in 10 mM NaCl (mV)[b]	-19.8 ± 4.0	-20.5 ± 2.7	-34.7 ± 7.1*	-55.6 ± 6.1*
Zeta potential in PM (mV)[b]	-11.3 ± 6.5	-13.7 ± 5.8	-11.9 ± 11.2	-13.9 ± 7.4

Abbreviations: DD double distilled; PM perfusion medium; TEM transmission electron microscopy

[a]according to the manufacturer's information; [b]experimentally determined (mean ± SD); [c]experimentally determined (mode ± SD); [d]calculated values; (*) $p<0.05$ compared to the plain beads of the same size.

Figure Legends

Figure 1. Particle size distribution (A, B) and TEM analysis (C - F) of the PS beads. Size distribution of plain (A) and carboxylate-modified (B) PS beads was measured in DD water (solid line) and PM (dashed line) by nanoparticle tracking analysis. (C – F) TEM micrographs of plain 50 nm (C), plain 240 nm (D), carboxylate-modified 50 nm (E) and carboxylate-modified 300 nm (F) polystyrene beads in DD water. The inserts in the upper left hand corner show a higher magnification of the PS beads. Arrow indicates an additional fraction of smaller PS beads.

Figure 2. Perfusion profiles and transfer rates of PS beads during *ex vivo* human placental perfusion. Transplacental transport of plain (A) and carboxylate-modified (B) PS beads over a time period of 6 hrs either from the maternal to fetal (M to F) or reverse from the fetal to maternal (F to M) circulation (C and D). Initially 25 µg/mL beads were added to the maternal (normal perfusions; continuous line) or fetal (reverse perfusions; dashed line) circulation, respectively. The amount of particles was determined by fluorescence measurement in the maternal (M, solid symbols) and fetal (F, open symbols) circuit at several time points. Data represents the mean particle concentration ± SD of at least 3 independent experiments. Transfer of PS beads calculated after 6 hrs of perfusion (E). Data is expressed as mean percentage of the initially added amount of PS beads ± SD of at least 3 independent experiments. (*) $p < 0.05$, (**) $p < 0.01$, (***) $p < 0.001$.

Figure 3. Localization (A, B) and quantification (C) of PS beads in the placental tissue. (A) Fluorescence microscope images of placental tissue after 6 hrs of perfusion in normal and reverse direction with plain 50 nm, plain 240 nm, carboxylate-modified 50 nm and carboxylate-modified 300 nm PS beads (green). Nuclei were stained with DAPI (blue). (B) Fluorescence microscope images of placental tissue before and after control perfusions without particles. (C) Theoretical NP tissue content after 6 hrs of perfusion. Displayed is the percentage of initially added PS beads after subtraction of the PS fractions in fetal and maternal circuits after 6 hrs (mean ± SD of at least 3 independent experiments). *ST: syncytiotrophoblast; S: Stroma; FC: fetal capillary; MB: maternal blood space).* (*) $p < 0.05$, (***) $p < 0.001$

Environ Health Perspect doi: 10.1289/ehp.1409271
Advance Publication: Not Copyedited

Figure 1.

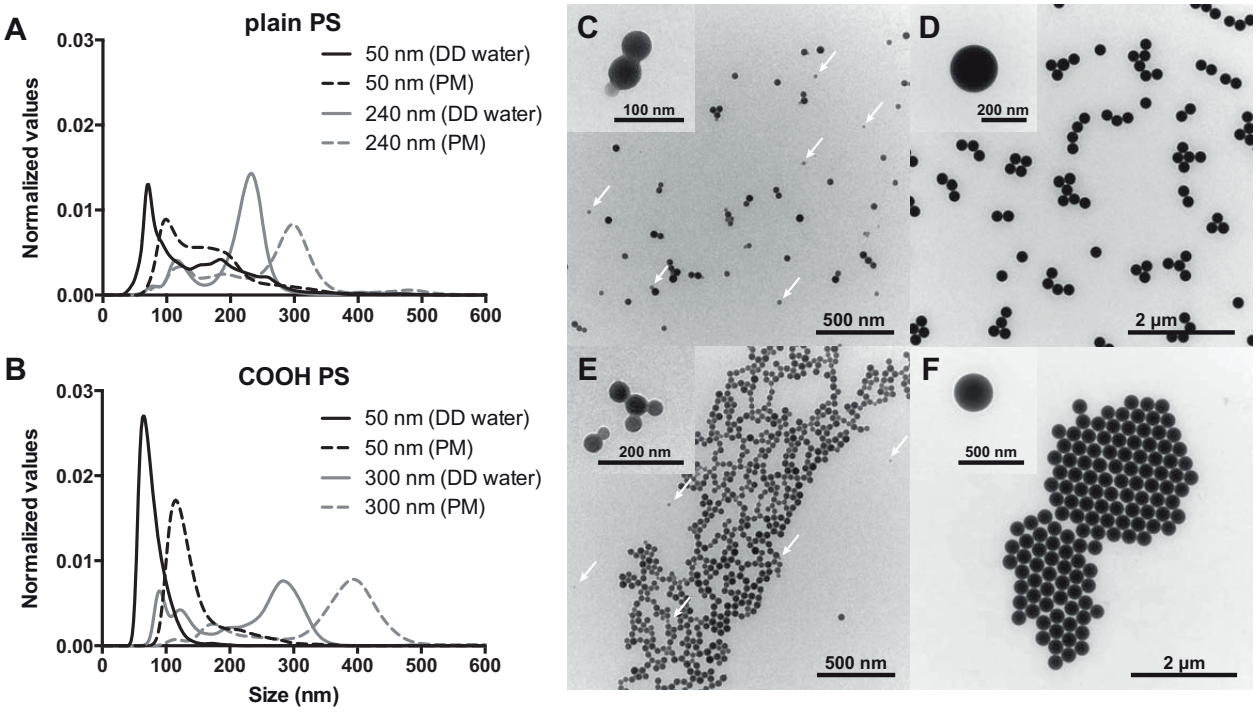

Figure 2.

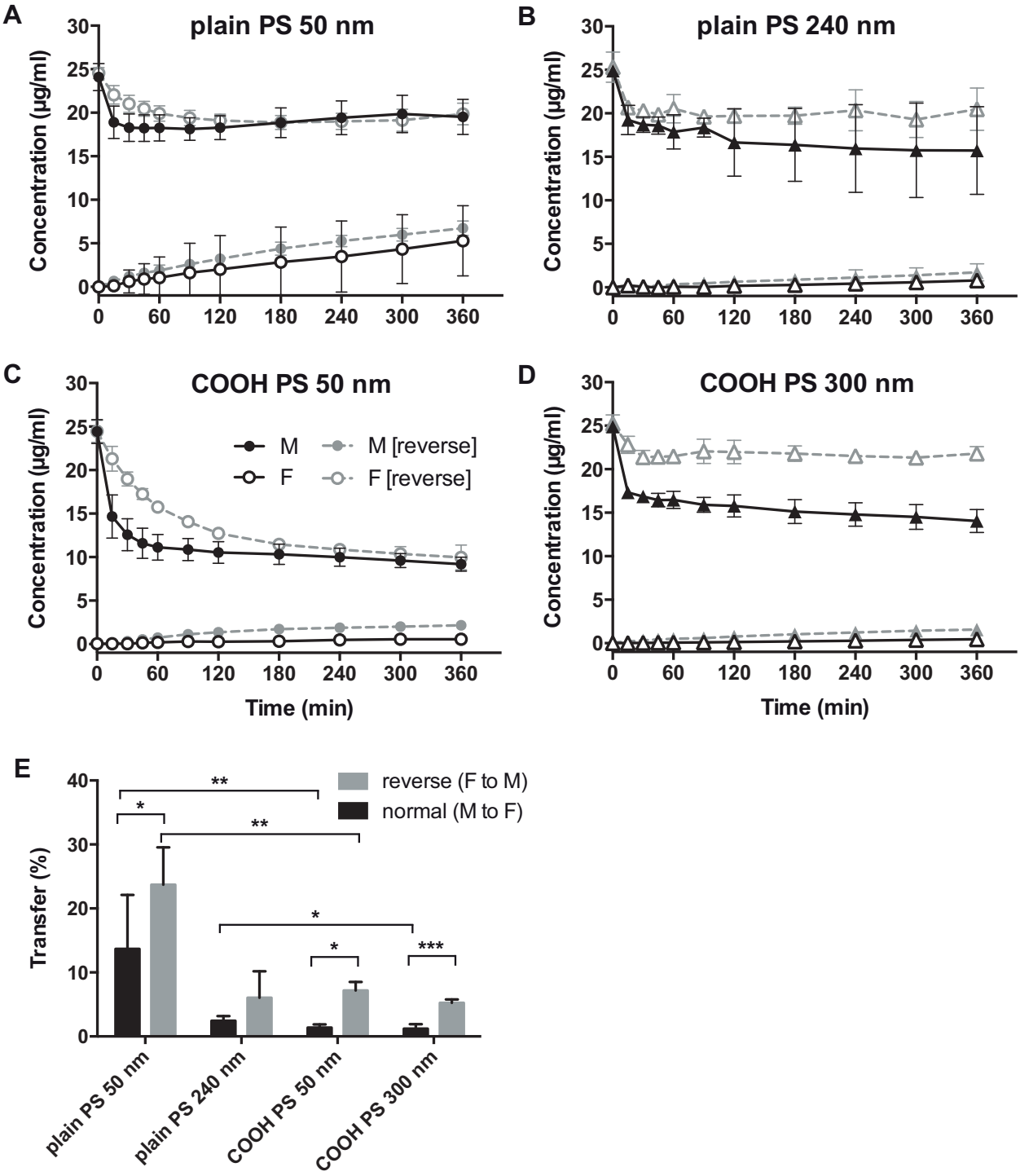
A
plain PS 50 nm
B
plain PS 240 nm
C
COOH PS 50 nm
D
COOH PS 300 nm
Concentration (µg/ml)
Time (min)
M
F
M [reverse]
F [reverse]
E
reverse (F to M)
normal (M to F)
Transfer (%)
plain PS 50 nm
plain PS 240 nm
COOH PS 50 nm
COOH PS 300 nm

Figure 3.

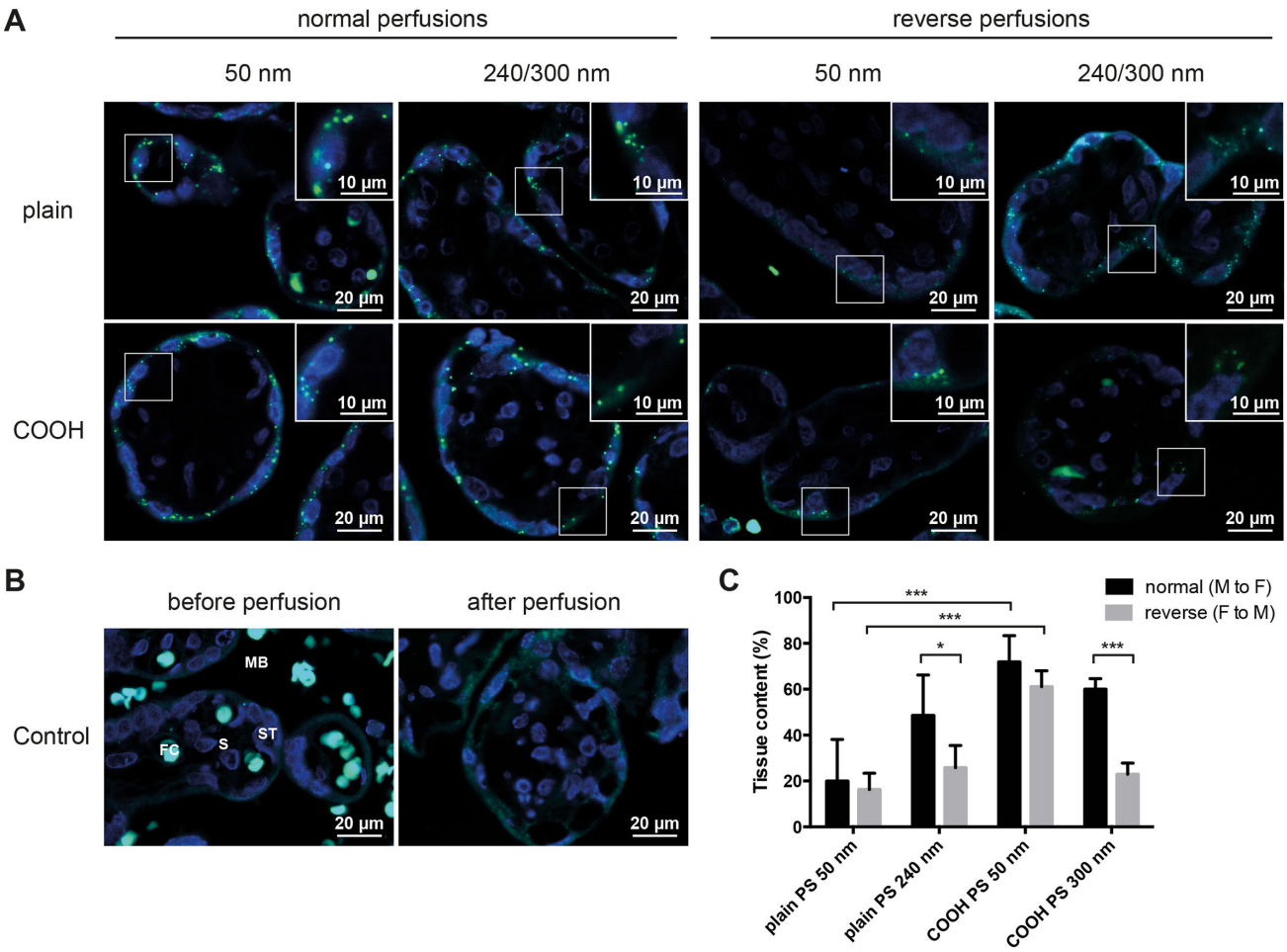
A
normal perfusions
reverse perfusions
50 nm
240/300 nm
50 nm
240/300 nm
plain
COOH
10 µm
20 µm
B
before perfusion
after perfusion
Control
MB
ST
FC
S
20 µm
C
normal (M to F)
reverse (F to M)
Tissue content (%)
100
80
60
40
20
0
***
***
*
***
plain PS 50 nm
plain PS 240 nm
COOH PS 50 nm
COOH PS 300 nm